Enhancement of secondary aerosol formation by reduced anthropogenic emissions during Spring Festival 2019 and enlightenment for regional $PM_{2.5}$ control in Beijing

Yuying Wang[1], Zhanqing Li[2], Qiuyan Wang[1], Xiaoai Jin[3], Peng Yan[4], Maureen Cribb[2], Yanan Li[4], Cheng Yuan[1], Hao Wu[3], Tong Wu[3], Rongmin Ren[3], Zhaoxin Cai[3]

[1]Key Laboratory for Aerosol-Cloud-Precipitation of China Meteorological Administration, School of Atmospheric Physics, Nanjing University of Information Science & Technology, Nanjing 210044, China

[2]Earth System Science Interdisciplinary Center, Department of Atmospheric and Oceanic Science, University of Maryland, College Park, MD, USA

[3]State Key Laboratory of Remote Sensing Science, College of Global Change and Earth System Science, Beijing Normal University, Beijing 100875, China

[4]CMA Meteorological Observation Center, Centre for Atmosphere Watch and Services, Beijing 100081, China

Correspondence to: Yuying Wang (yuyingwang@nuist.edu.cn)

Abstract

A comprehensive field experiment measuring aerosol chemical and physical properties at a suburban site in Beijing around the 2019 Spring Festival was carried out to investigate the impact of reduced anthropogenic emissions on aerosol formation. Sharply reduced sulfur dioxide (SO_2) and nitrogen dioxide (NO_2) concentrations during the festival holiday resulted in an unexpected increase in the surface ozone (O_3) concentration caused by the strong O_3-titration phenomenon. Simultaneously, the reduced anthropogenic emissions resulted in massive decreases in particle number concentration at all sizes and the mass concentrations of organics and black carbon. However, the mass concentrations of inorganics (especially sulfate) decreased weakly. Detailed analyses of the sulfur oxidation ratio and the nitrogen oxidation ratio suggest that sulfate formation during the holiday could be promoted by enhanced nocturnal aqueous-phase chemical reactions between SO_2 and O_3 under moderate relative humidity (RH) conditions (40 % < RH < 80 %). Daytime photochemical reactions in winter in Beijing mainly controlled nitrate formation, which was enhanced a little during the holiday. A regional analysis of air pollution patterns shows that the enhanced formation of secondary aerosols occurred throughout the entire Beijing-Tian-Hebei (BTH) region during the holiday, partly offsetting the decrease in particle matter with an aerodynamic diameter less than 2.5 μm. Our results highlight the necessary control of O_3 formation to reduce secondary pollution in winter under current emission conditions.

1. Introduction

Aerosols consist of liquid and solid particles, and their mixture suspended in the atmosphere. The massive increase in aerosol particles caused by human activities in urban areas (e.g., traffic, industrial production, and construction work) can deteriorate air quality to the point of having a detrimental impact on human health (e.g., Chow et al., 2006; Matus et al., 2012; Gao et al., 2017; Zhong et al., 2018; An et al., 2019). Moreover, aerosols can change atmospheric optical and hygroscopic properties, altering the transfer of solar radiation and the development of clouds, thereby changing weather and climate in both aerosol source regions and their downstream areas (e.g., Altaratz et al., 2014; R. Zhang et al., 2015; Z. Li et al., 2016, 2019; Y. Wang et al., 2018, 2019b; Jin et al., 2020).

With the rapid economic development and urbanization in recent decades in China, the scales of many cities have expanded quickly along with sharply increased populations in urban areas, especially in the three most economically developed regions (the Beijing-Tianjin-Hebei (BTH) metropolitan region, the Yangtze River Delta, and the Pearl River Delta). As a result, air pollution has become a severe problem in these megacity regions (e.g., Chan and Yao, 2008; Han et al., 2014; Zhong et al., 2018). On some heavy haze days, the mass concentration of particulate matter with an aerodynamic diameter of less than 2.5 μm ($PM_{2.5}$) dramatically increased from tens to hundreds of micrograms per cubic meter in several hours (Guo et al., 2014; Sun et al., 2016a).

Over the past a few years, many emission control measures have been taken in

China to mitigate air pollution. As a response, the mass concentration of $PM_{2.5}$ has decreased in most cities in China since 2013, especially in the BTH region (Q. Zhang et al., 2019; Vu et al., 2019; Zhai et al., 2019). Organics and black carbon (BC) concentrations largely decreased during these years thanks to the reduction in coal combustion and biomass burning (H. Li et al., 2019a; Xu et al., 2019). Simultaneously, the mass concentrations of inorganics (mainly sulfate, nitrate, and ammonium) also decreased due to the reduction in their gaseous precursors (especially sulfur dioxide, or SO_2). However, the mass fraction of inorganics increased by more than 10 % during these years (H. Li et al., 2019a; Y. Wang et al., 2019a), implying the enhancement of secondary inorganic aerosol (SIA) formation, which partly counteracted the decrease in $PM_{2.5}$. All these variations would change aerosol physicochemical properties. For example, Xie et al. (2020) found that the aerosol pH increased as $PM_{2.5}$ decreased in the past few years in urban Beijing due to the enhanced mass ratio of nitrate to sulfate. As a possible consequence of the elevated aerosol pH, the dissolved ozone (O_3) in particles would play a more important role to SIA formation, especially for sulfate formation (Seinfeld and Pandis, 2016). Therefore, the major chemical processes during haze events and the control target should be re-evaluated. Elaborating the secondary aerosol formation mechanism under current emission conditions is important for taking more proper measures to control $PM_{2.5}$ in the future.

Some studies have argued that controlling emissions of nitrogen oxides (NO_x) is important because nitrate in $PM_{2.5}$ has had the weakest decrease relative to other chemical species over the past several years (Q. Zhang et al., 2019; F. Zhang et al.,

2020). The transformation of NO_x to nitrate is closely related to atmospheric oxidation processes (Seinfeld and Pandis, 2016). Surface ozone (O_3) is an important secondary gaseous pollutant and oxidizing agent in the atmosphere. Recent studies have found that a reduction in $PM_{2.5}$ resulted in an increase in the O_3 volume mixing ratio ([O_3]) at a rate of 3.3 ppbv per annum during the summer of the past few years in the BTH region (K. Li et al., 2019, 2020). The increased [O_3] can enhance the atmospheric oxidation capacity, thereby promoting the formation of secondary aerosols in summer (T. Wang et al., 2017). However, less emphasis has been placed on the variation in [O_3] in winter. The formation of O_3 and its effect on secondary aerosol formation in a cold environment is thus unclear.

Some special events held in China have provided unique opportunities to investigate the impact of human activities on air quality by taking advantage of unusual changes associated with short-term, drastic measures implemented by the Chinese government to reduce anthropogenic emissions, such as the 2008 Summer Olympic Games (T. Wang et al., 2010; Guo et al., 2013), the 2014 Asia-Pacific Economic Cooperation (Sun et al., 2016b), the 2015 China Victory Day parade (Y. Wang et al., 2017; Zhao et al., 2017), and the 2016 G20 Summit (H. Li et al., 2019b). The annual Spring Festival holiday is also a special occasion when the vast majority of the population stops working for 2 to 4 weeks (Tan et al., 2009; Y. Zhang et al., 2016; C. Wang et al., 2017). Investigating the impact of changes in anthropogenic emissions on gaseous pollutants and aerosol formation during these special occasions may provide useful guidance on more scientifically sound measures to take to control $PM_{2.5}$.

A comprehensive aerosol field experiment at a suburban site near the 5th Ring Road in the Daxing District of Beijing was carried out for more than two years, including the 2019 Spring Festival. Beijing was one of the three top cities in China with the largest migrating population during the 2019 Spring Festival holiday (https://cloud.tencent.com/developer/news/393324). In addition, fireworks were prohibited throughout the Beijing metropolitan region within the 6th Ring of the Beijing Beltway. The intensity of anthropogenic emissions was thus much weaker than usual during this holiday. Our measurements around this period of the field campaign are thus ideal for investigating the impact of reduced anthropogenic emissions on surface O_3 and aerosol formation.

This paper is structured as follows. Section 2 describes the experiment site and the measurement data used in this study. Section 3 presents the results and discussion, mainly concerning the impact of reduced anthropogenic emissions during the holiday on the variations in trace gases and aerosol chemical species in Beijing and the BTH region. Section 4 presents the conclusions and their implications.

2. Experiment site and measurement data

A comprehensive field experiment measuring aerosol physical and chemical properties was conducted from August 2017 to October 2019 at a suburban site in southern Beijing (Fig. 1). Note that this study only employs measurements made around the 2019 Spring Festival from 16 January to 17 February. This site (39.81°N, 116.48°E) is the test center for meteorological instruments constructed by the China

Meteorological Administration (CMA). It is surrounded by Beijing's 5th Ring Road, industrial parks, and residential communities (Fig. S1). Aerosol chemical and physical properties in this area are thus mainly anthropogenic, varying considerably around the time of the festival in response to the full cycle of industrial activities as the majority of people stopped and resumed working. This provides an opportunity to investigate the impact of reduced anthropogenic emissions on surface O_3 and aerosol formation processes in winter.

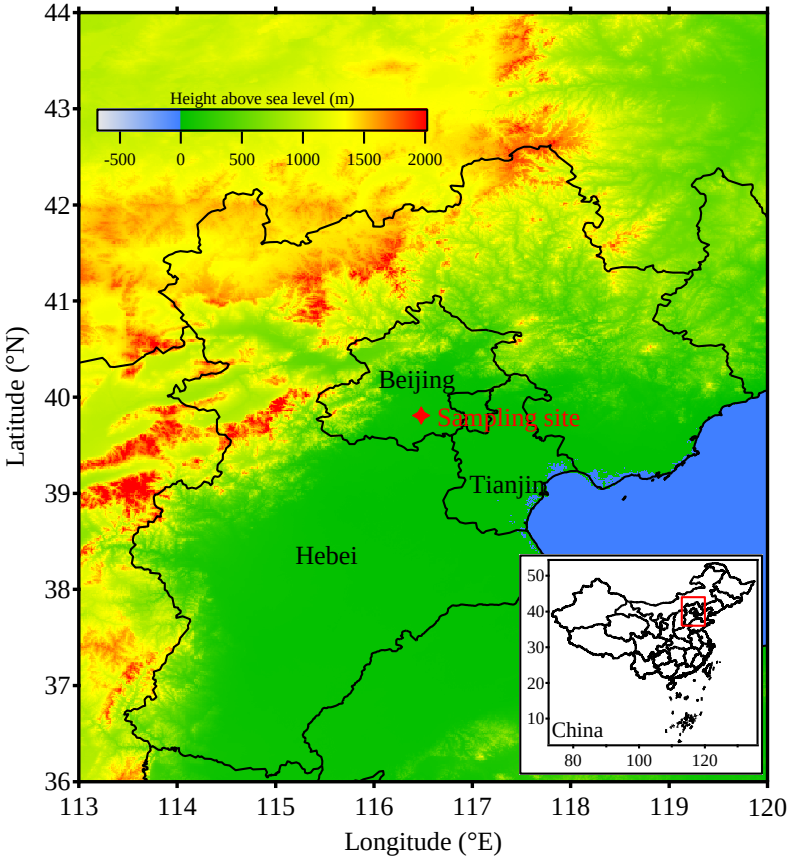

Figure 1. Map showing the Beijing-Tianjin-Hebei region in China and the location of the experiment site. The colored background shows the terrain height (unit: m above sea level).

Table 1 lists the instruments used in this campaign. A scanning mobility particle sizer (SMPS) and an aerodynamic particle sizer (APS) measured the aerosol particle number size distribution (PNSD) from 10 nm to 20 μm. The SMPS consists of a differential mobility analyzer (model 3081, TSI Inc.) and a condensation particle counter (model 3772, TSI Inc.). The aerodynamic diameter measured by the APS can be converted to the Stokes diameter through division by the square root of the aerosol density. The aerosol density in this study was calculated following the method of Zhao et al. (2017), using measured aerosol chemical composition information. An aerosol chemical speciation monitor (ACSM) equipped with a $PM_{2.5}$ lens system, a capture vaporizer, and a quadrupole mass spectrometer was used to measure mass concentrations of non-refractory aerosol chemical species in $PM_{2.5}$, including organics (Org), nitrate (NO_3^-), sulfate (SO_4^{2-}), ammonium (NH_4^+), and chlorine (Chl) (Peck et al., 2016; Xu et al., 2017; Y. Zhang et al., 2017). A seven-wavelength aethalometer (model AE-33, Magee Scientific Corp.) with a $PM_{2.5}$ cyclone in the sample inlet was used to retrieve the mass concentration of BC.

In addition to the above aerosol measurements, meteorological parameters were observed by the CMA at the experiment site. The Chinese Ministry of Ecology and Environment network and Beijing Municipal Environmental Monitoring Center (http://106.37.208.233:20035/ and http://www.bjmemc.com.cn/) provided $PM_{2.5}$ and trace gas (sulfur dioxide (SO_2), nitrogen dioxide (NO_2), carbon monoxide (CO), and O_3) measurements made in different locations of the BTH region. Yizhuang in Beijing is the nearest station to the experiment site (about 3.0 km to the southeast, Fig. S1). The

total mass concentrations of measured non-refractory aerosol chemical species and BC mass concentrations in $PM_{2.5}$ show good consistency with the $PM_{2.5}$ mass concentrations obtained from the Yizhuang station (Fig. S2).

Table 1. Aerosol instruments used in this campaign and their observed parameters and manufacturer information.

Instrument	Measured Parameters	Manufacturer	Model	Time Resolution
SMPS	Particle number size distribution (10–550 nm)	TSI	3938	5 min
APS	Particle number size distribution (0.5–20 μm)	TSI	3321	5 min
ACSM	Mass concentrations of non-refractory aerosol chemical species in $PM_{2.5}$	Aerodyne	Q-ACSM	15 min
Aethalometer	Mass concentration of black carbon	Magee	AE-33	5 min

3. Results and Discussion

3.1. Basic meteorological and environmental characteristics

While the official Spring Festival holiday was from 4 February to 10 February 2019, many people left before 3 February and came back after the Lantern Festival (19 February). In this study, we regarded the days from 16 January to 2 February as the polluted (POL) period with high anthropogenic emissions, more representative of ordinary conditions, and the days from 3 February to 17 February as the background (BG) period with low anthropogenic emissions. Figure 2 shows the time series of meteorological parameters, trace gas volume mixing ratios, and aerosol properties during the two periods.

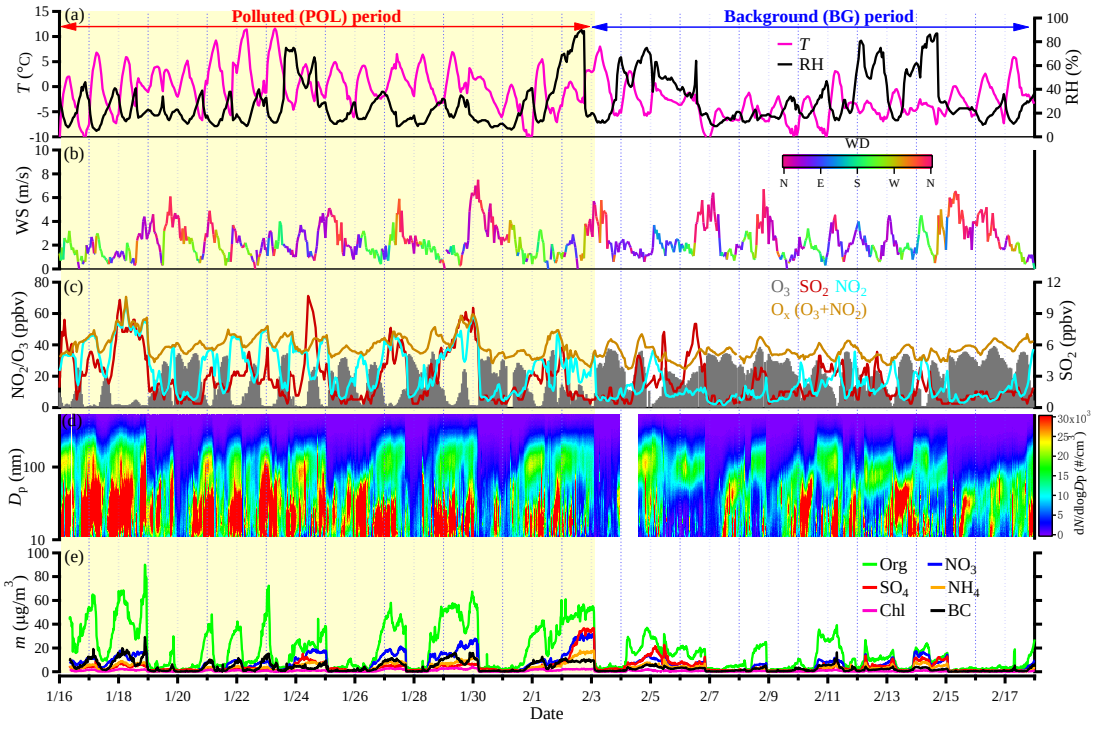

Figure 2. Time series of (**a**) ambient temperature (*T*) and relative humidity (RH), (**b**) wind direction (WD) and speed (WS), (**c**) volume mixing ratios of trace gases [O_3, SO_2, NO_2 and O_x (O_3+NO_2)], (**d**) the aerosol particle number size distribution measured by the SMPS, and (**e**) mass concentrations of aerosol chemical species in $PM_{2.5}$ measured by the ACSM and the AE-33. The trace gas information was from the Yizhuang station, and the others were observed at the experiment site in Beijing (16 January to 17 February 2019).

Ambient temperature (*T*) and relative humidity (RH) have clear diurnal cycles (Fig. 2a). The average *T* and RH during the BG period were slightly lower (-3.3±3.4 versus 0.2±4.2°C) and higher (33.2±20.1 versus 25.8±17.6 %) than those during the POL period, respectively. This was caused by several short-term light snowfall events that

178 occurred on 6, 12, and 14 February during the BG period. Figures 2b and S3 display
179 similar wind patterns during the POL and BG periods, i.e., wind patterns that changed
180 periodically. The prevailing, strong northerly winds during the two periods were
181 beneficial to dispersing pollutants in Beijing (Sun et al., 2016b; Y. Wang et al., 2017),
182 and thus no heavy haze episodes occurred during these periods. Overall, the
183 meteorological parameters were similar during the POL and BG periods.

184 Figure 2c illustrates that the volume mixing ratios of SO_2 and NO_2 ([SO_2] and
185 [NO_2]) during the BG period were lower than those during the POL period, suggesting
186 less gaseous pollutants from anthropogenic emissions during the BG period. In
187 addition, [O_3] remained at a high level for several days during the BG period but not
188 during the POL period. The average [O_3] increased by 77.4 % during the BG period
189 compared with the POL period (46.2±18.9 versus 26.1±22.2 ppbv). The percent change
190 in [O_3] due to the "holiday effect" during this field campaign is much higher than that
191 reported in other regions of China (K. Huang et al., 2012; C. Wang et al., 2017; S. Wang
192 et al., 2019). Figure 2c also shows a weak variation in O_x (O_3 + NO_2) from the POL
193 period to the BG period, indicating that strong O_3-titration appeared during the Spring
194 Festival 2019.

195 Many bursts of fine particles (Fig. 2d) occurring mainly during rush hours or at
196 night were observed during the POL period. This is likely related to the substantial
197 increases in gasoline or diesel vehicles on two nearby roads at these times. Zhu et al.
198 (2017) found that efficient nucleation and partitioning of gaseous species from on-road
199 vehicles can promote new particle formation in the wintertime. However, this

200 phenomenon occurred much less frequently during the BG period, likely because of the
201 massive reduction in on-road vehicles. The few short-term bursts of fine particles
202 during the BG period occurred during the daytime, presumably because of enhanced
203 nucleation by photochemical processes.

204 The aerosol chemical species in $PM_{2.5}$ also differed during the POL and BG periods
205 (Fig. 2e). During the POL period, the mass concentrations of aerosol chemical species
206 readily accumulated, especially the organics (m_{org}) with rapid increases at night. The
207 mass concentration of BC (m_{BC}) also clearly increased, likely associated with an
208 increase in heavy-duty diesel vehicles and a decrease in the nocturnal planetary
209 boundary layer at night (Y. Wang et al., 2017; Zhao et al., 2017; Z. Li et al., 2017).
210 However, the increases in m_{org} and m_{BC} at night during the BG period were not as strong
211 as those during the POL period. The mass concentration of nitrate (m_{NO3}) largely
212 decreased during the BG period, while there was a weak variation in the mass
213 concentration of sulfate (m_{SO4}).

214 In summary, distinct differences existed in all observed trace gases and aerosol
215 chemical and physical parameters during the POL and BG periods. However, the
216 meteorological parameters (wind direction and speed, ambient temperature, and RH)
217 and weather regimes were similar during these two periods. This helps to single out the
218 impact of reduced anthropogenic emissions on trace gases and aerosol formation
219 processes.

220

221 **3.2. Impact of reduced anthropogenic emissions on aerosol formation processes**

The average $PM_{2.5}$ mass concentrations were 46.3 and 22.5 μg/m^3 during the POL and BG periods, respectively. Figure 3 illustrates the average PNSD and aerosol chemical species in $PM_{2.5}$ during the two periods. The particle number concentrations at all sizes were much higher during the POL period than during the BG period, especially for ultrafine particles (with diameters, or D_p, < 100 nm). The diurnal variation in PNSD during the POL period shown in Fig. 4a suggests that aerosol particles with D_p < 50 nm burst during rush hours and in the nighttime. The total particle number concentration (N) remained greater than 30,000 cm^{-3} at these times. However, during the BG period, the number concentration of ultrafine particles only increased weakly during rush hours or nucleation times. N was always less than 20,000 cm^{-3} on all days during the BG period (Fig. 4b), probably linked with the reduction in on-road vehicles during the holiday. As shown in Table 2, the ratio of BG to POL 10–50 nm particle number concentrations ($N_{10–50\ nm}$) (0.47) is much smaller than the ratios for larger particles (0.78 for $N_{50–100\ nm}$ and 0.67 for $N_{>100\ nm}$). These all demonstrate the strong impact of reduced anthropogenic emissions on aerosol number concentrations, especially for nucleation-mode and small Aitken-mode particles.

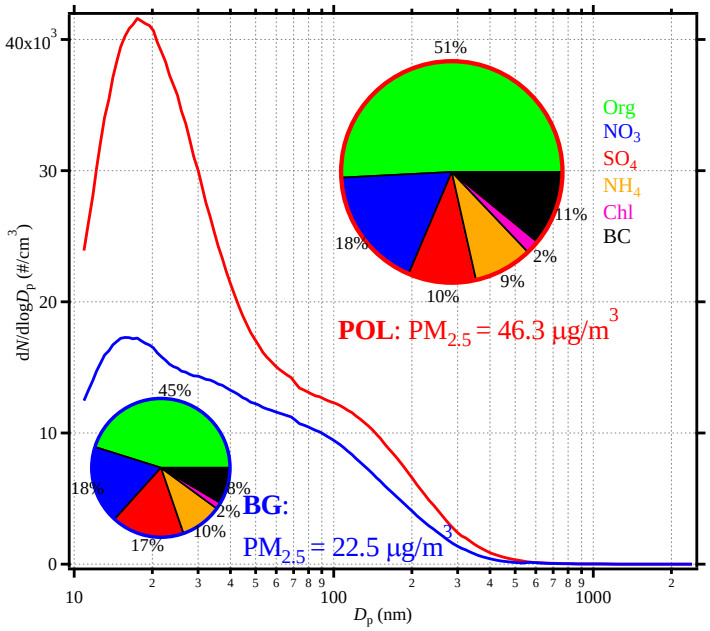

239

240 **Figure 3.** Average aerosol particle number size distributions (red and blue curves) and

241 mass fractions of aerosol chemical species in $PM_{2.5}$ (pie charts with red and blue

242 outlines) during the POL (in red) and BG (in blue) periods.

243

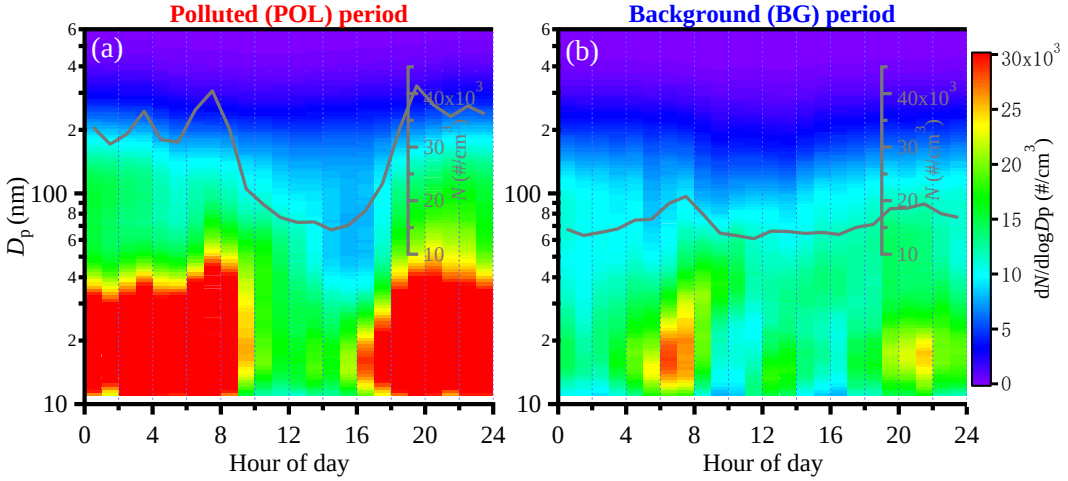

244

245 **Figure 4**. Diurnal variations in aerosol particle number size distribution (colored

246 background) and total aerosol number concentration (*N*, shown as grey curves) during

247 the (**a**) POL and (**b**) BG periods.

248

Table 2. Summary of the average aerosol number concentration (N) in different size ranges, volume mixing ratios of trace gases, mass concentrations of $PM_{2.5}$ and different aerosol chemical species, sulfur oxidation ratios (SOR), and nitrogen oxidation ratios (NOR) during the POL and BG periods and their ratios.

	$N_{10-50\ nm}$ (cm^{-3})	$N_{50-100\ nm}$ (cm^{-3})	$N_{>100\ nm}$ (cm^{-3})	SO_2 （ppbv）	NO_2 （ppbv）	O_3 （ppbv）	$PM_{2.5}$ （μg/m³）
POL	20,861±19,935	3,946±2,544	3,888±2,757	8.31±6.35	51.96±27.35	26.06±22.24	46.32±39.05
BG	9,837±8,493	3,071±1,478	2,600±2,223	4.85±3.83	21.87±13.99	46.23±18.86	22.52±20.28
BG/POL	0.47	0.78	0.67	0.58	0.42	1.77	0.49
	m_{Org} (μg/m³)	m_{NO3} (μg/m³)	m_{SO4} (μg/m³)	m_{NH4} (μg/m³)	m_{BC} (μg/m³)	SOR	NOR
POL	23.55±19.58	8.25±7.91	4.59±6.20	3.96±3.83	5.05±4.51	0.27±0.17	0.09±0.08
BG	10.17±9.13	4.09±4.25	3.82±4.08	2.18±2.14	1.91±1.74	0.32±0.18	0.10±0.08
BG/POL	0.43	0.50	0.83	0.55	0.38	1.19	1.11

Table 2 also indicates that the mass concentrations (m) of aerosol chemical species in $PM_{2.5}$ were much less during the BG period than during the POL period . The m related to primary emissions (m_{org} and m_{BC}) decreased by more than 50 %, but the m of secondary inorganic aerosols (SIA, including nitrate, sulfate, and ammonium) slightly decreased, especially sulfate (m_{SO4} decreased by only 17 %). The pie charts in Fig. 3 show significant differences in the aerosol chemical species of $PM_{2.5}$ during the two periods. The mass fractions of Org and BC were lower during the BG period (45 % and 8 %, respectively) than during the POL period (51 % and 11 %, respectively). By contrast, the mass fraction of SIA was higher during the BG period (45 %) than during the POL period (37 %). This indicates that the strongly reduced anthropogenic emissions during the holiday caused sharp decreases in primary aerosols but not secondary aerosols. The sulfur oxidation ratio (SOR) and nitrogen oxidation ratio (NOR) are usually calculated to study the transformation of secondary aerosols

(Sun et al., 2006; Y. Li et al., 2017). SOR (NOR) is defined as the ratio of the molar concentration of sulfate (nitrate) to the total molar concentration of sulfate (nitrate) and SO_2 (NO_2). Table 2 shows that SOR and NOR were higher during the BG period than during the POL period, suggesting that the formation of secondary inorganics was enhanced during the BG period. Figure 5 shows that most large $PM_{2.5}$ mass concentrations (> 100 μg/m^3) during the POL period occurred along with low RH (< 40 %) and low SIA mass fractions, indicating the important contribution of primary emissions to the accumulation of $PM_{2.5}$ in a polluted environment. However, large $PM_{2.5}$ mass concentrations (> 50 μg/m^3) during the BG period mainly appeared under moderate RH (40 < RH < 80 %) and high SIA mass fraction conditions, likely caused by enhanced aqueous-phase chemical reactions during this period.

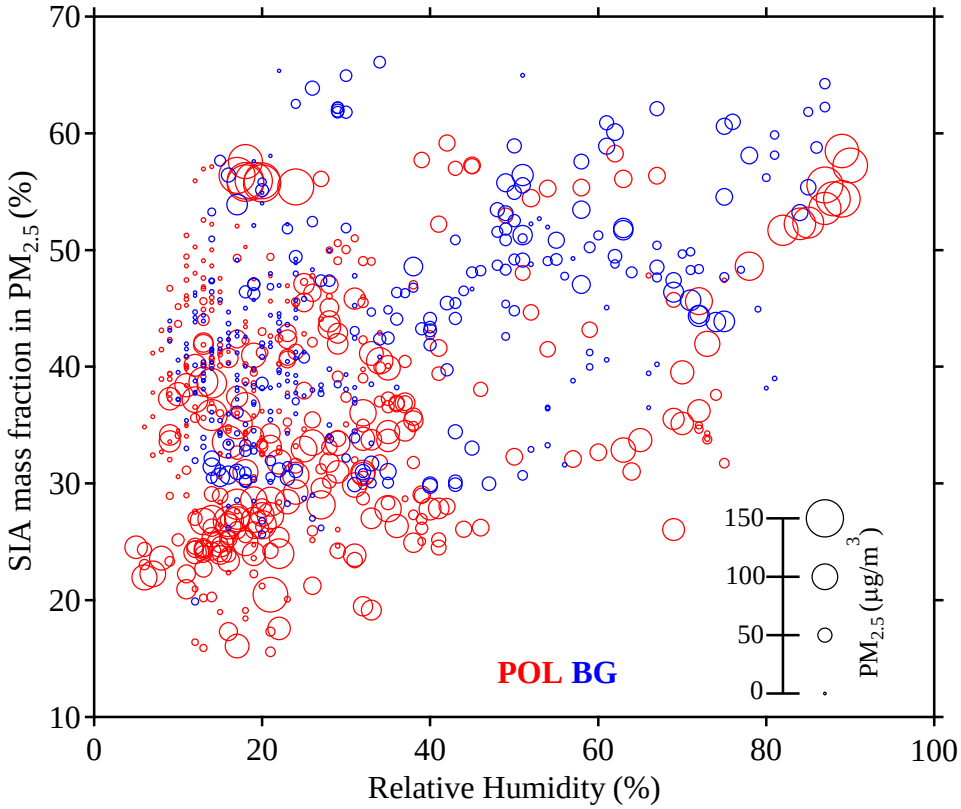

Figure 5. The variation in secondary inorganic aerosols (SIA) mass fraction in $PM_{2.5}$ as a function of ambient relative humidity during the POL (in red) and BG (in blue) periods. The different circle sizes denote different $PM_{2.5}$ mass concentrations.

The diurnal variation in $[O_3]$ (Fig. 6a) shows more accumulated O_3 during the BG period than during the POL period at any time of the day. In particular, $[O_3]$ at night was two times higher during the BG period than during the POL period (Fig. 6b). Distinct diurnal variations in SOR were found during the two periods (Fig. 6c). The higher SOR at night during the BG period (Fig. 6c) indicates the enhanced transformation of SO_2 to sulfate, likely related to nocturnal aqueous-phase chemical reactions due to the elevated ambient RH at night (Fig. S4). Figure S5 indicates that SOR increased following an increase in ALWC when the ambient RH was higher than

~40 % during the BG period. Moreover, Fig. 6d shows that the diurnal variation in the SOR ratio during the two periods was similar to that of the [O_3] ratio. This suggests that sulfate formation during the holiday was likely enhanced by nocturnal aqueous-phase chemical reactions between SO_2 and O_3. This is consistent with the study of Fang et al. (2019), which found that ambient RH and the O_3 concentration are two prerequisites for rapid sulfate formation via aqueous-phase oxidation reactions. This result highlights that controlling O_3 formation under current emission conditions in winter in Beijing is key to further reducing the formation of sulfate and implies that the high underestimation of sulfate at night in models (Miao et al., 2020) could be caused by an inaccurate simulation of [O_3]. The higher daytime NOR (Fig. 6e) than nighttime NOR during the two periods illustrates that the formation of nitrate was mainly controlled by photochemical reactions in winter. Figure 6f shows that the larger NOR difference (the higher NOR ratio) during rush hours during the two periods likely occurred because a mass of emitted NO_x during rush hours could not be transformed to nitrate during the POL period. Figure 6e and 6f also suggests nitrate formation was somewhat enhanced during the holiday likely due to enhanced daytime photochemical reactions.

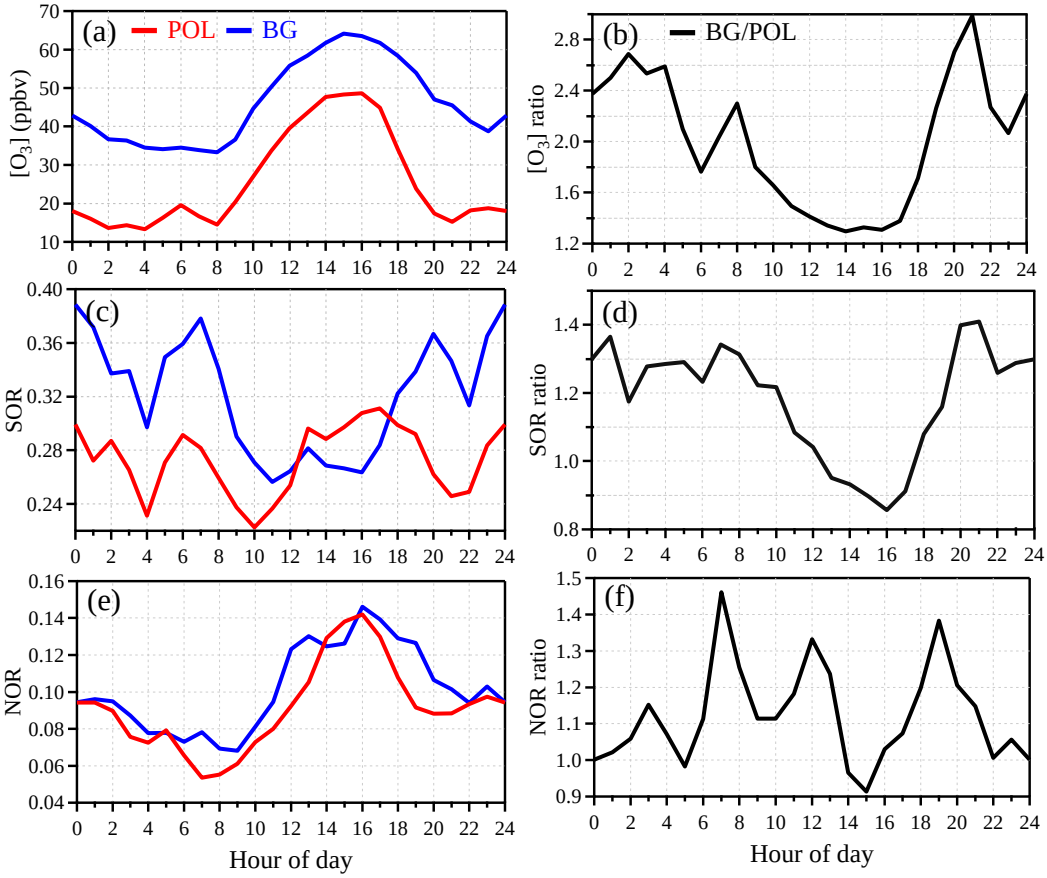

Figure 6. Diurnal variations in (**a** and **b**) O_3 volume mixing ratio and its ratio, (**c** and **d**) sulfur oxidation ratio (SOR) and its ratio, and (**e** and **f**) nitrogen oxidation ratio (NOR) and its ratio during the BG and POL periods. The ratio of a quantity is that quantity during the BG period divided by that quantity during the POL period.

Overall, the reduced anthropogenic emissions led to a drastic decrease in aerosol particle number concentration during the holiday. However, the general enhancement of [O_3] could promote the formation of secondary inorganics (especially sulfate).

3.3. Impact of reduced anthropogenic emissions on regional air pollution

Figure 7a-c shows that the volume mixing ratios of emitted trace gases ([SO_2], [NO_2], and [CO]) decreased in the Bejing-Tianjin-Hebei (BTH) region during the BG period. [NO_2] and [SO_2] decreased by more than 40 % in all cities and 35 % in heavy-industry cities (distributed in the southern and northeastern parts of the BTH region). This indicates a regional reduction in anthropogenic emissions during the holiday. Figure 7d shows that [O_3] increased in all cities and that the increase was more than 50 % in all cities except for a high-altitude city (Zhangjiakou) to the northwest.

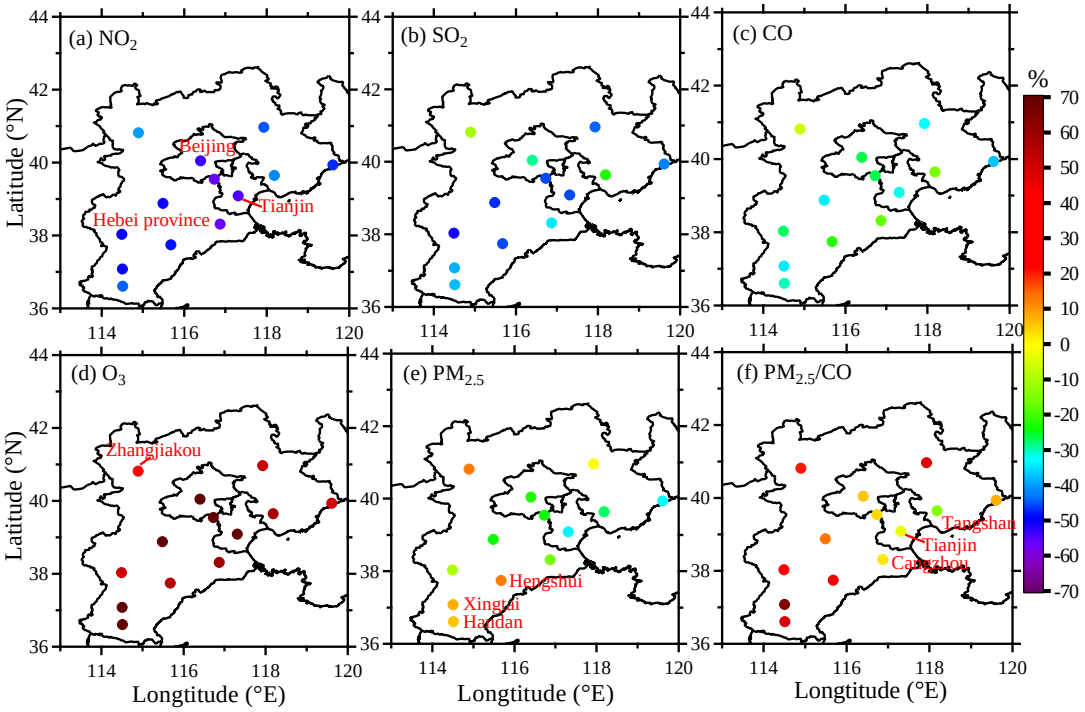

Figure 7. Percent changes in trace gas volume mixing ratios (NO_2, SO_2, CO, and O_3), the $PM_{2.5}$ mass concentration, and the $PM_{2.5}$/CO ratio during the BG period relative to the POL period: $100 \times \left(\frac{[BG]-[POL]}{[POL]}\right)$ in the Beijing-Tianjin-Hebei (BTH) region.

The $PM_{2.5}$ mass concentration decreased at a much lower rate relative to the decrease in [NO_2] and [SO_2] in most cities during the BG period (Fig. 7e), while it

increased slightly at Zhangjiakou and three southern heavy-industry cities (Hengshui, Xingtai, and Handan). The ratio $PM_{2.5}$/CO is an indicator of aerosol secondary formation to primary emissions. An increase in $PM_{2.5}$/CO was found during the BG period at all cities except for three coastal cities (Tangshan, Tianjin, and Cangzhou), revealing the regional enhancement of secondary aerosol formation during the holiday. The weak decrease in $PM_{2.5}$/CO at the three coastal cities was likely due to the influence of mixed sea flows.

The regional analysis of air pollution assumes that the findings from Beijing presented in section 3.2 are applicable to the entire BTH region. Regionally reduced anthropogenic emissions resulted in sharply decreased gaseous pollutants and increased O_3. The enhanced formation of secondary aerosols likely due to enhanced aqueous chemical reactions involving O_3 could counteract the decrease in $PM_{2.5}$ mass concentration. There are two possible reasons explaining the high [O_3] during the holiday: (1) the reduced gaseous precursors (NO_x and SO_2) weakened the consumption of O_3, and (2) O_3 formation in the BTH region is likely volatile organic compound (VOC)-controlled under current emission conditions, therefore the reduction in NO_x would lead to higher [O_3]. All these results demonstrate that it is important to reduce O_3 formation to further control $PM_{2.5}$ in winter in the BTH region.

4. Conclusions and Implications

In recent years, the mass concentration of particulate matter with an aerodynamic

diameter of less than 2.5 μm ($PM_{2.5}$) has shown a general decreasing trend, presumably due to the series of emission reduction measures taken in China in an attempt to improve air quality. However, haze pollution episodes still occur from time to time, including during some special events when primary emissions reduced drastically, such as the Chinese New Year holiday and even during the COVID-19 lockdown when anthropogenic activities diminished dramatically (X. Huang et al., 2020). We conjecture that reductions through primary emissions may be offset by increases in the formation of secondary aerosols.

To test this, we examined the secondary aerosol formation mechanism in a comprehensive field experiment conducted in Beijing. Aerosol and meteorological measurements were made for more than two years, but data around the 2019 Chinese Spring Festival from 16 January to 17 February were employed in this study to single out the impact of emission reductions due to the holiday. The study period was divided into polluted (POL) and background (BG) periods, with high and low anthropogenic emissions before and during the festival holiday, respectively. Investigated were the impacts of reduced anthropogenic emissions on trace gases and $PM_{2.5}$ under similar meteorological conditions.

The average $PM_{2.5}$ mass concentrations were 46.3 and 22.5 $\mu g/m^3$ during the POL and BG periods, respectively, with no heavy haze events occurring. The average aerosol particle number size distribution shows that the reduced anthropogenic emissions during the holiday led to decreased aerosol number concentrations at all sizes, especially in the nucleation and Aitken modes (mobility diameters less than 50 nm).

Simultaneously, the reduced anthropogenic emissions resulted in decreases in the volume mixing ratios of SO_2 and NO_2 and an unexpected increase in the volume mixing ratio of O_3 [O_3] during the BG period caused by the appeared O_3-titration phenomenon. The analysis of the aerosol chemical species in $PM_{2.5}$ demonstrates that the large decreases in organics and black carbon mass concentrations during the BG period were likely caused by the large decrease in on-road vehicles. Moreover, the mass concentration of nitrate also decreased while that of sulfate decreased much less during the BG period. Comparisons of the sulfur oxidation ratio (SOR) and the nitrogen oxidation ratio (NOR) during the two periods imply that the transformation of gaseous precursors to secondary inorganics (especially the transformation of SO_2 to sulfate) was promoted during the BG period, likely due to the enhanced aqueous chemical reactions involving the dissolved O_3. The diurnal variation in the SOR ratio between the BG and POL periods was similar to that of the [O_3] ratio, illustrating that sulfate formation was promoted by the enhanced nocturnal aqueous-phase chemical reactions between SO_2 and O_3 under moderate relative humidity (RH) conditions (40 % < RH < 80 %). The higher NOR in the daytime during the two periods points out that the formation of nitrate was mainly controlled by photochemical reactions and weakly affected by the increase in [O_3].

This study also investigated the impact of reduced anthropogenic emissions on regional air pollution patterns during the holiday. The variation trends of trace gases in most cities in the Beijing-Tian-Hebei (BTH) region were similar to those in Beijing, indicating the regional influence of reduced anthropogenic emissions on the volume

mixing ratios of trace gases during the holiday. The weak $PM_{2.5}$ variation and the increased $PM_{2.5}$/CO ratio (an indicator of aerosol secondary formation to primary emissions) during the BG period both suggest that the enhanced formation of secondary aerosols offset the regional decrease in $PM_{2.5}$ during the holiday.

Our findings provide evidence that decreases in anthropogenic emissions can promote the formation of secondary inorganics due to the enhancement of aqueous reactions likely caused by the increased [O_3]. This result implies that haze mitigation in north China needs a coordinated and balanced strategy for controlling multiple pollutants.

Acknowledgement. This work was funded by the National Key R&D Program of the Ministry of Science and Technology, China (grant no. 2017YFC1501702), the National Natural Science Foundation of China (NSFC) research project (grant no. 42005067), and the Open Fund of State Key Laboratory of Remote Sensing Science (grant no. 202015).

Data availability. Data from the Chinese Ministry of Ecology and Environment network and Beijing Municipal Environmental Monitoring Center can be downloaded from the websites given in the main text. The measurement data from the field experiment used in this study are available from the first author upon request (yuyingwang@nuist.edu.cn).

Author contributions. ZL and PY designed the field experiment. YW and ZL conceived the study and led the overall scientific questions. YW, QW, and XJ

processed the measurement data and prepared this paper. MC copyedited the article. Other co-authors participated in the implementation of this experiment and the discussion of this paper.

Competing interests. The authors declare that they have no conflict of interest.

References

Altaratz, O., Koren, I., Remer, L. A., and Hirsch, E.: Review: Cloud invigoration by aerosols—coupling between microphysics and dynamics, Atmos. Res., 140, 38–60, https://doi.org/10.1016/j.atmosres.2014.01.009, 2014.

An, Z., Huang, R., Zhang, R., Tie, X., Li, G., Cao, J., Zhou, W., Shi, Z., Han, Y., Gu, Z., and Ji, Y.: Severe haze in northern China: a synergy of anthropogenic emissions and atmospheric processes, Proc. Natl. Acad. Sci. U.S.A., 116, 8657, https://doi.org/10.1073/pnas.1900125116, 2019.

Chan, C. K., and Yao, X.: Air pollution in megacities in China, Atmos. Environ., 42, 1–42, https://doi.org/10.1016/j.atmosenv.2007.09.003, 2008.

Chow, J. C., Watson, J. G., Mauderly, J. L., Costa, D. L., Wyzga, R. E., Vedal, S., Hidy, G. M., Altshuler, S. L., Marrack, D., Heuss, J. M., Wolff, G. T., Arden Pope III, C., and Dockery, D. W.: Health effects of fine particulate air pollution: lines that connect, J. Air Waste Manage., 56, 1368–1380, https://doi.org/10.1080/10473289.2006.10464545, 2006.

Fang, Y., Ye, C., Wang, J., Wu, Y., Hu, M., Lin, W., Xu, F., and Zhu, T.: Relative humidity and O_3 concentration as two prerequisites for sulfate formation, Atmos. Chem. Phys., 19, 12,295–12,307, https://doi.org/10.5194/acp-19-12295-2019, 2019.

Gao, J., Woodward, A., Vardoulakis, S., Kovats, S., Wilkinson, P., Li, L., Xu, L., Li, J., Yang, J., Li, J., Cao, L., Liu, X., Wu, H., and Liu, Q.: Haze, public health and mitigation measures in China: a review of the current evidence for further policy response, Sci. Total Environ., 578, 148–157, https://doi.org/10.1016/j.scitotenv.2016.10.231, 2017.

Guo, S., Hu, M., Guo, Q., Zhang, X., Schauer, J. J., and Zhang, R.: Quantitative evaluation of emission controls on primary and secondary organic aerosol sources during Beijing 2008 Olympics, Atmos. Chem. Phys., 13, 8303–8314, https://doi.org/10.5194/acp-13-8303-2013, 2013.

Guo, S., Hu, M., Zamora, M. L., Peng, J., Shang, D., Zheng, J., Du, Z., Wu, Z., Shao, M., Zeng, L., Molina, M. J., and Zhang, R.: Elucidating severe urban haze formation in China, Proc. Natl. Acad. Sci. U.S.A., 111, 17373, https://doi.org/10.1073/pnas.1419604111, 2014.

Han, L., Zhou, W., Li, W., and Li, L.: Impact of urbanization level on urban air quality: a case of fine particles ($PM_{2.5}$) in Chinese cities, Environ. Pollut., 194, 163–170, https://doi.org/10.1016/j.envpol.2014.07.022, 2014.

Huang, K., Zhuang, G., Lin, Y., Wang, Q., Fu, J. S., Zhang, R., Li, J., Deng, C., and Fu, Q.: Impact of anthropogenic emission on air quality over a megacity revealed from an intensive atmospheric

campaign during the Chinese Spring Festival, Atmos. Chem. Phys., 12, 11,631–11,645, https://doi.org/10.5194/acp-12-11631-2012, 2012.

Huang, X., Ding, A., Gao, J., Zheng, B., Zhou, D., Qi, X., Tang, R., Wang, J., Ren, C., Nie, W., Chi, X., Xu, Z., Chen, L., Li, Y., Che, F., Pang, N., Wang, H., Tong, D., Qin, W., Cheng, W., Liu, W., Fu, Q., Liu, B., Chai, F., Davis, S. J., Zhang, Q. and He, K.: Enhanced secondary pollution offset reduction of primary emissions during COVID-19 lockdown in China, National Science Review, https://doi.org/ 10.1093/nsr/nwaa137, 2020.

Jin, X., Wang, Y., Li, Z., Zhang, F., Xu, W., Sun, Y., Fan, X., Chen, G., Wu, H., Ren, J., Wang, Q., and Cribb, M.: Significant contribution of organics to aerosol liquid water content in winter in Beijing, China, Atmos. Chem. Phys., 20, 901–914, https://doi.org/10.5194/acp-20-901-2020, 2020.

Li, H., Cheng, J., Zhang, Q., Zheng, B., Zhang, Y., Zheng, G., and He, K.: Rapid transition in winter aerosol composition in Beijing from 2014 to 2017: response to clean air actions, Atmos. Chem. Phys., 19, 11,485–11,499, https://doi.org/10.5194/acp-19-11485-2019, 2019a.

Li, H., Wang, D., Cui, L., Gao, Y., Huo, J., Wang, X., Zhang, Z., Tan, Y., Huang, Y., Cao, J., Chow, J. C., Lee, S., and Fu, Q.: Characteristics of atmospheric $PM_{2.5}$ composition during the implementation of stringent pollution control measures in shanghai for the 2016 G20 summit, Sci. Total Environ., 648, 1121–1129, https://doi.org/10.1016/j.scitotenv.2018.08.219, 2019b.

Li, K., Jacob, D. J., Liao, H., Shen, L., Zhang, Q., and Bates, K. H.: Anthropogenic drivers of 2013–2017 trends in summer surface ozone in China, P. Natl. Acad. Sci. U.S.A., 116, 422–427, https://doi.org/10.1073/pnas.1812168116, 2019.

Li, K., Jacob, D. J., Shen, L., Lu, X., De Smedt, I., and Liao, H.: 2013–2019 increases of surface ozone pollution in China: anthropogenic and meteorological influences, Atmos. Chem. Phys. Discuss., 2020, 1–18, https://doi.org/10.5194/acp-2020-298, 2020.

Li, Y. J., Sun, Y., Zhang, Q., Li, X., Li, M., Zhou, Z., and Chan, C. K.: Real-time chemical characterization of atmospheric particulate matter in China: a review, Atmos. Environ., 158, 270–304, https://doi.org/10.1016/j.atmosenv.2017.02.027, 2017.

Li, Z., Lau, W. K. M., Ramanathan, V., Wu, G., Ding, Y., Manoj, M. G., Liu, J., Qian, Y., Li, J., Zhou, T., Fan, J., Rosenfeld, D., Ming, Y., Wang, Y., Huang, J., Wang, B., Xu, X., Lee, S. S., Cribb, M., Zhang, F., Yang, X., Zhao, C., Takemura, T., Wang, K., Xia, X., Yin, Y., Zhang, H., Guo, J., Zhai, P. M., Sugimoto, N., Babu, S. S., and Brasseur, G. P.: Aerosol and monsoon climate interactions over Asia, Rev. Geophys., 54, 866–929, https://doi.org/10.1002/2015RG000500, 2016.

Li, Z., Guo, J., Ding, A., Liao, H., Liu, J., Sun, Y., Wang, T., Xue, H., Zhang, H., and Zhu, B.: Aerosol and boundary-layer interactions and impact on air quality, Natl. Sci. Rev., 4, 810–833, https://doi.org/10.1093/nsr/nwx117, 2017.

Li, Z., Wang, Y., Guo, J., Zhao, C., Cribb, M. C., Dong, X., Fan, J., Gong, D., Huang, J., Jiang, M., Jiang, Y., Lee, S. S., Li, H., Li, J., Liu, J., Qian, Y., Rosenfeld, D., Shan, S., Sun, Y., Wang, H., Xin, J., Yan, X., Yang, X., Yang, X., Zhang, F., and Zheng, Y.: East Asian Study of Tropospheric Aerosols and their Impact on Regional Clouds, Precipitation, and Climate (EAST-AIRCPC), J. Geophys. Res. Atmos., 124, 13,026–13,054, https://doi.org/10.1029/2019JD030758, 2019.

Matus, K., Nam, K., Selin, N. E., Lamsal, L. N., Reilly, J. M., and Paltsev, S.: Health damages from air pollution in China, Global Environ. Change, 22, 55–66, https://doi.org/10.1016/j.gloenvcha.2011.08.006, 2012.

Miao, R., Chen, Q., Zheng, Y., Cheng, X., Sun, Y., Palmer, P. I., Shrivastava, M., Guo, J., Zhang, Q., Liu, Y., Tan, Z., Ma, X., Chen, S., Zeng, L., Lu, K., and Zhang, Y.: Model bias in simulating major

chemical components of $PM_{2.5}$ in China, Atmos. Chem. Phys. Discuss., 2020, 1–33, https://doi.org/10.5194/acp-2020-76, 2020.

Peck, J., Gonzalez, L. A., Williams, L. R., Xu, W., Croteau, P. L., Timko, M. T., Jayne, J. T., Worsnop, D. R., Miake-Lye, R. C., and Smith, K. A.: Development of an aerosol mass spectrometer lens system for $PM_{2.5}$, Aerosol Sci. Tech., 50, 781–789, https://doi.org/10.1080/02786826.2016.1190444, 2016.

Seinfeld, J. H., and Pandis, S. N.: Atmospheric chemistry and physics: from air pollution to climate change, edited, John Wiley & Sons, 2016.

Sun, Y., Zhuang, G., Tang, A., Wang, Y., and An, Z.: Chemical characteristics of $PM_{2.5}$ and PM_{10} in haze-fog episodes in Beijing, Environ. Sci. Technol., 40, 3148–3155, https://doi.org/10.1021/es051533g, 2006.

Sun, Y., Chen, C., Zhang, Y., Xu, W., Zhou, L., Cheng, X., Zheng, H., Ji, D., Li, J., Tang, X., Fu, P., and Wang, Z.: Rapid formation and evolution of an extreme haze episode in Northern China during winter 2015, Sci. Rep.-UK, 6, https://doi.org/10.1038/srep27151, 2016a.

Sun, Y., Wang, Z., Wild, O., Xu, W., Chen, C., Fu, P., Du, W., Zhou, L., Zhang, Q., Han, T., Wang, Q., Pan, X., Zheng, H., Li, J., Guo, X., Liu, J., and Worsnop, D. R.: "APEC Blue": secondary aerosol reductions from emission controls in Beijing, Sci. Rep.-UK, 6, 20668, https://doi.org/10.1038/srep20668, 2016b.

Tan, P., Chou, C., Liang, J., Chou, C. C. K., and Shiu, C.: Air pollution "holiday effect" resulting from the Chinese New Year, Atmos. Environ., 43, 2114–2124, https://doi.org/10.1016/j.atmosenv.2009.01.037, 2009.

Vu, D., Gao, S., Berte, T., Kacarab, M., Yao, Q., Vafai, K., and Asa-Awuku, A.: External and internal cloud condensation nuclei (CCN) mixtures: controlled laboratory studies of varying mixing states, Atmos. Meas. Tech., 12, 4277–4289, https://doi.org/10.5194/amt-12-4277-2019, 2019.

Wang, C., Huang, X. F., Zhu, Q., Cao, L. M., Zhang, B., and He, L. Y.: Differentiating local and regional sources of Chinese urban air pollution based on the effect of the Spring Festival, Atmos. Chem. Phys., 17, 9103–9114, https://doi.org/10.5194/acp-17-9103-2017, 2017.

Wang, S., Yu, R., Shen, H., Wang, S., Hu, Q., Cui, J., Yan, Y., Huang, H., and Hu, G.: Chemical characteristics, sources, and formation mechanisms of $PM_{2.5}$ before and during the Spring Festival in a coastal city in Southeast China, Environ. Pollut., 251, 442–452, https://doi.org/10.1016/j.envpol.2019.04.050, 2019.

Wang, T., Nie, W., Gao, J., Xue, L. K., Gao, X. M., Wang, X. F., Qiu, J., Poon, C. N., Meinardi, S., Blake, D., Wang, S. L., Ding, A. J., Chai, F. H., Zhang, Q. Z., and Wang, W. X.: Air quality during the 2008 Beijing Olympics: secondary pollutants and regional impact, Atmos. Chem. Phys., 10, 7603–7615, https://doi.org/10.5194/acp-10-7603-2010, 2010.

Wang, T., Xue, L., Brimblecombe, P., Lam, Y. F., Li, L., and Zhang, L.: Ozone pollution in China: a review of concentrations, meteorological influences, chemical precursors, and effects, Sci. Total Environ., 575, 1582–1596, https://doi.org/10.1016/j.scitotenv.2016.10.081, 2017.

Wang, Y., Zhang, F., Li, Z., Tan, H., Xu, H., Ren, J., Zhao, J., Du, W., and Sun, Y.: Enhanced hydrophobicity and volatility of submicron aerosols under severe emission control conditions in Beijing, Atmos. Chem. Phys., 17, 5239–5251, https://doi.org/10.5194/acp-17-5239-2017, 2017.

Wang, Y., Li, Z., Zhang, Y., Du, W., Zhang, F., Tan, H., Xu, H., Fan, T., Jin, X., Fan, X., Dong, Z., Wang, Q., and Sun, Y.: Characterization of aerosol hygroscopicity, mixing state, and CCN activity at a suburban site in the central North China Plain, Atmos. Chem. Phys., 18, 11,739–11,752, https://doi.org/10.5194/acp-18-11739-2018, 2018.

Wang, Y., Chen, J., Wang, Q., Qin, Q., Ye, J., Han, Y., Li, L., Zhen, W., Zhi, Q., Zhang, Y., and Cao, J.: Increased secondary aerosol contribution and possible processing on polluted winter days in China, Environ. Int., 127, 78–84, https://doi.org/10.1016/j.envint.2019.03.021, 2019a.

Wang, Y., Li, Z., Zhang, R., Jin, X., Xu, W., Fan, X., Wu, H., Zhang, F., Sun, Y., Wang, Q., Cribb, M., and Hu, D.: Distinct ultrafine- and accumulation-mode particle properties in clean and polluted urban environments, Geophys. Res. Lett., 46, 10,918–10,925, 10.1029/2019GL084047, 2019b.

Xie, Y., Wang, G., Wang, X., Chen, J., Chen, Y., Tang, G., Wang, L., Ge, S., Xue, G., Wang, Y., and Gao, J.: Nitrate-dominated $PM_{2.5}$ and elevation of particle pH observed in urban Beijing during the winter of 2017, Atmos. Chem. Phys., 20, 5019-5033, 10.5194/acp-20-5019-2020, 2020.

Xu, W., Croteau, P., Williams, L., Canagaratna, M., Onasch, T., Cross, E., Zhang, X., Robinson, W., Worsnop, D., and Jayne, J.: Laboratory characterization of an aerosol chemical speciation monitor with $PM_{2.5}$ measurement capability, Aerosol Sci. Tech., 51, 69–83, https://doi.org/10.1080/02786826.2016.1241859, 2017.

Xu, W., Sun, Y., Wang, Q., Zhao, J., Wang, J., Ge, X., Xie, C., Zhou, W., Du, W., Li, J., Fu, P., Wang, Z., Worsnop, D. R., and Coe, H.: Changes in aerosol chemistry from 2014 to 2016 in winter in Beijing: insights from high-resolution aerosol mass spectrometry, J. Geophys. Res. Atmos., 124, 1132–1147, https://doi.org/10.1029/2018JD029245, 2019.

Zhai, S., Jacob, D. J., Wang, X., Shen, L., Li, K., Zhang, Y., Gui, K., Zhao, T., and Liao, H.: Fine particulate matter ($PM_{2.5}$) trends in China, 2013–2018: separating contributions from anthropogenic emissions and meteorology, Atmos. Chem. Phys., 19, 11,031–11,041, https://doi.org/10.5194/acp-19-11031-2019, 2019.

Zhang, F., Wang, Y., Peng, J., Chen, L., Sun, Y., Duan, L., Ge, X., Li, Y., Zhao, J., Liu, C., Zhang, X., Zhang, G., Pan, Y., Wang, Y., Zhang, A. L., Ji, Y., Wang, G., Hu, M., Molina, M. J., and Zhang, R.: An unexpected catalyst dominates formation and radiative forcing of regional haze, Proc. Natl. Acad. Sci. U.S.A., 117, 3960, https://doi.org/10.1073/pnas.1919343117, 2020.

Zhang, Q., Zheng, Y., Tong, D., Shao, M., Wang, S., Zhang, Y., Xu, X., Wang, J., He, H., Liu, W., Ding, Y., Lei, Y., Li, J., Wang, Z., Zhang, X., Wang, Y., Cheng, J., Liu, Y., Shi, Q., Yan, L., Geng, G., Hong, C., Li, M., Liu, F., Zheng, B., Cao, J., Ding, A., Gao, J., Fu, Q., Huo, J., Liu, B., Liu, Z., Yang, F., He, K., and Hao, J.: Drivers of improved $PM_{2.5}$ air quality in China from 2013 to 2017, P. Natl. Acad. Sci. U.S.A., 116, 24,463–24,469, https://doi.org/10.1073/pnas.1907956116, 2019.

Zhang, R., Wang, G., Guo, S., Zamora, M. L., Ying, Q., Lin, Y., Wang, W., Hu, M., and Wang, Y.: Formation of urban fine particulate matter, Chem. Rev., 115, 3803–3855, https://doi.org/10.1021/acs.chemrev.5b00067, 2015.

Zhang, Y., Sun, Y., Du, W., Wang, Q., Chen, C., Han, T., Lin, J., Zhao, J., Xu, W., Gao, J., Li, J., Fu, P., Wang, Z., and Han, Y.: Response of aerosol composition to different emission scenarios in Beijing, China, Sci. Total Environ., 571, 902–908, https://doi.org/10.1016/j.scitotenv.2016.07.073, 2016.

Zhang, Y., Tang, L., Croteau, P. L., Favez, O., Sun, Y., Canagaratna, M. R., Wang, Z., Couvidat, F., Albinet, A., Zhang, H., Sciare, J., Prévôt, A. S. H., Jayne, J. T., and Worsnop, D. R.: Field characterization of the $PM_{2.5}$ aerosol chemical speciation monitor: insights into the composition, sources, and processes of fine particles in eastern China, Atmos. Chem. Phys., 17, 14,501–14,517, https://doi.org/10.5194/acp-17-14501-2017, 2017.

Zhao, J., Du, W., Zhang, Y., Wang, Q., Chen, C., Xu, W., Han, T., Wang, Y., Fu, P., Wang, Z., Li, Z., and Sun, Y.: Insights into aerosol chemistry during the 2015 China Victory Day parade: results from simultaneous measurements at ground level and 260 m in Beijing, Atmos. Chem. Phys., 17, 3215–

3232, https://doi.org/10.5194/acp-17-3215-2017, 2017.
Zhong, S., Qian, Y., Sarangi, C., Zhao, C., Leung, R., Wang, H., Yan, H., Yang, T., and Yang, B.: Urbanization effect on winter haze in the Yangtze River Delta Region of China, Geophys. Res. Lett., 45, 6710–6718, https://doi.org/10.1029/2018GL077239, 2018.
Zhu, Y., Yan, C., Zhang, R., Wang, Z., Zheng, M., Gao, H., Gao, Y., and Yao, X.: Simultaneous measurements of new particle formation at 1-s time resolution at a street site and a rooftop site, Atmos. Chem. Phys., 17, 9469–9484, https://doi.org/10.5194/acp-17-9469-2017, 2017.